On the behaviour of magnetostrictive amorphous ribbons in low magnetic fields

1995 J. Phys.: Condens. Matter 7 1689

(http://iopscience.iop.org/0953-8984/7/8/015)

J. Phys.: Condens. Matter 7 (1995) 1689–1699. Printed in the UK

On the behaviour of magnetostrictive amorphous ribbons in low magnetic fields

I Ciobotaru and N Rezlescu
Institute of Technical Physics Iasi, D Mangeron 47, Iasi 6600, Romania

Received 6 April 1994, in final form 26 October 1994

Abstract. A phenomenological model is proposed for the magnetoelastic behaviour at low fields for an amorphous ribbon that has been field annealed in the ribbon plane at an arbitrary angle to the sample axis. The model takes into account the anisotropy energy, the Zeeman energy, the domain coupling energy, the shape energy and the effects of the pinned wall and charged wall. Explicit expressions for the initial susceptibility and quadratic coefficients of engineering magnetostriction are obtained.

1. Introduction

Some amorphous ribbons present large values of the magnetomechanical coupling coefficient and the properties of soft magnetic material. That is why they are used in the production of sensors and transducers. For devices working in low magnetic fields, it is useful to model their magnetic and magnetoelastic behaviour depending on such parameters as applied stress and field-annealing angle.

The dependence of the initial susceptibility on the applied stress and the field-annealing angle has been analysed considering only the rotation process [1,2] or both rotation and displacement processes [3]. These models describe correctly the dependence of the initial susceptibility χ on the direction of the easy axis of the magnetization for the special cases of transverse or longitudinal anisotropy.

The model proposed in [4] for the isotropic material starts from the concept of pseudodomains with pinned walls and takes into account the interdomain coupling interaction. The domain coupling energy explicitly depends on the strains; this leads to an expression for the magnetostriction differing from that used in [1–3].

The field-annealed amorphous ribbons are characterized by a well defined easy axis and a small constant of intrinsic anisotropy.

The model suggested by Squire [3] starts from the domain pattern of the field-annealed amorphous ribbons and takes into account the effects of intrinsic anisotropy, magnetoelastic anisotropy, wall displacement and applied field.

In the present work a phenomenological model is proposed to describe the low-field behaviour of field-annealed amorphous ribbons. The model starts from the Squire [3] model and also includes the effects of shape, interdomain coupling interactions (because of the change in direction, inside the domain, the divergence of the vector of local magnetization is non-zero and hence magnetostatic interactions will be present) and magnetostatic interactions due to the magnetically charged walls (if the component of the domain magnetization M_D normal to the wall is not continuous, charges appear on the wall surface).

The expressions for the initial susceptibility χ, and the quadratic coefficients of engineering magnetostriction c_q and C_Q are obtained, starting from the free energy.

0953-8984/95/081689+11$19.50

2. Theory

2.1. Domain coupling energy

Let us consider a sample field annealed in the ribbon plane at an angle ϵ_0 to the sample axis. Under the influence of a magnetic field parallel to the sample axis, the magnetization vectors M_{D1} and M_{D2} from two joining domains will form the angles θ_1 and θ_2 with the ribbon axis and the wall will displace and rotate, forming an angle γ (figure 1). In the case of the pinned wall, $\gamma = \epsilon$. The volume fraction where the domain magnetization M_{D1} makes the angle θ_1 will become $v > 0.5$.

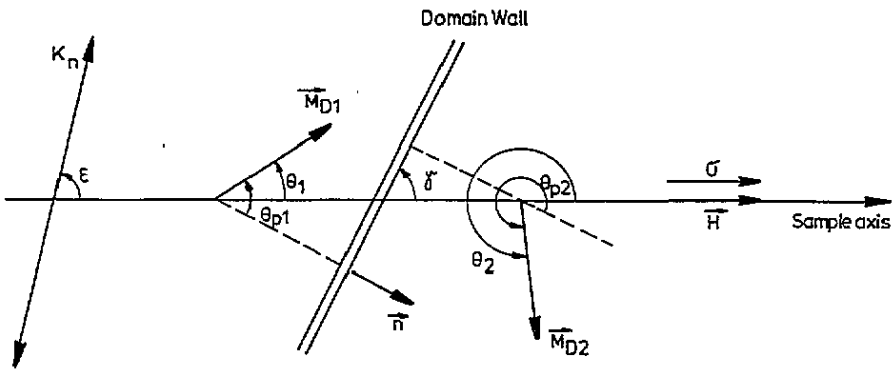

Figure 1. Domain pattern.

Owing to the chemical and topological disorder, the local anisotropy tensor shows spatial fluctuations. The direction of the magnetic moment is determined by the balance between the local anisotropy and exchange interactions [5]. This results in an average local domain magnetization M_D over which a moment direction distribution is superposed. In the field-annealed ribbons, the technical saturation M_D (for $H \simeq 10^2$–10^3 A m^{-1}) is lower than the saturation magnetization M_S (for $H \simeq 10^5$ A m^{-1}) [2]. Thus, for the whole technical magnetization region, there are spatial fluctuations in the magnetic moment direction. Because of the change in direction (inside the domain), the divergence of the vector of local magnetization is non-zero and hence magnetostatic interactions will be present (owing to the density of the volume pole) between the joining areas of the sample [6]. During the magnetization process, a change in the magnetic moment directions occurs, accompanied by a variation in the volume magnetostatic energy density E_V. For small values of the reduced magnetization m, one can suppose that

$$E_V = \alpha m^2 \tag{1}$$

where α is a parameter depending on the sample history. Taking into account the expression for the longitudinal m_l and transverse m_t components of the reduced magnetization given by

$$\begin{aligned} m_l &= v\cos\theta_1 + (1-v)\cos\theta_2 \\ m_t &= v\sin\theta_1 + (1-v)\sin\theta_2 \end{aligned} \tag{2}$$

one obtains

$$E_V \simeq \alpha \left[1 - 4v(1-v) \sin^2 \left(\frac{\theta_2 - \theta_1}{2} \right) \right]. \tag{3}$$

This expression was used in [7, 8] to describe the dependence of $\chi(\sigma)$ for the special cases $\epsilon_0 = 0$ and $\epsilon_0 = \pi/2$.

For high fields, the fluctuations diminish and the domain coupling energy decreases.

2.2. *Anisotropy*

Since the considered energy of magnetic domain coupling (section 2.1) is of magnetostatic origin (it does not depend on the deformation components, unlike the case treated in [4]), the equilibrium strains correspond to the minimum of the sum between the elastic and magnetoelastic energies (with respect to the strains).

When a longitudinal stress σ is applied, the anisotropy energy consists of two parts [3]: one due to the intrinsic anisotropy given by

$$E_{K_0} = K_0[v \sin^2(\epsilon_0 - \theta_1) + (1-v) \sin^2(\epsilon_0 - \theta_2)]$$

and the other due to the external stress given by

$$E_{K_\sigma} = K_\sigma[v \sin^2 \theta_1 + (1-v) \sin^2 \theta_2].$$

The magnetoelastic anisotropy constant K_σ is

$$K_\sigma = \tfrac{3}{2} \lambda_s \sigma$$

where λ_s is the saturation magnetostriction. The resultant anisotropy energy may be put into the form

$$E_K \equiv E_{K_0} + E_{K_\sigma} \equiv K[v \sin^2(\epsilon - \theta_1) + (1-v) \sin^2(\epsilon - \theta_2)] + \frac{K_0 + K_\sigma - K}{2}. \tag{4}$$

The resultant anisotropy constant K and the new direction of the easy axis ϵ are given by

$$\begin{aligned} K &= \sqrt{K_0^2 + K_\sigma^2 + 2K_0 K_\sigma \cos(2\epsilon_0)} \\ \tan(2\epsilon) &= \frac{K_0 \sin(2\epsilon_0)}{K_0 \cos(2\epsilon_0) + K_\sigma}. \end{aligned} \tag{5}$$

We note that the term $(K_0 + K_\sigma - K)/2$ does not depend on the domain wall position and the domain magnetization direction.

2.3. *Shape magnetostatic energy*

Let us consider an amorphous ribbon with the following dimensions: thickness $2d \simeq 20 \times 10^{-6}$ m; width $2b \simeq 2 \times 10^{-3}$ m; length $l \gg b$. Using the expression for the point function demagnetization factors (for a rectangular prism) given in [9], we find the volume average of the transverse demagnetization factor N_t and longitudinal demagnetization factor N_l.

$$N_t \simeq 8 \times 10^{-3}$$

$$N_l \ll N_t.$$

The shape magnetostatic energy will be

$$E_S = \alpha_t m_t^2 \tag{6}$$

where

$$\alpha_t = \tfrac{1}{2}\mu_0 N_t M_D^2. \tag{7}$$

From equation (7) and $\mu_0 M_D = 1.5$ T it is found that $\alpha_t \simeq 10^4$ J m^{-3}. Since $K_0 \simeq 10^2$ J m^{-3}, it follows that $\alpha_t \gg K_0$. Thus, owing to the shape effect, the transverse component of the technical magnetization will be zero.

A complication is the possibility that the direction of domain magnetization near the sample surface is changed by the surface free poles [10]. Because the ratio of the domain width to the sample thickness is greater than unity, the scalar potential Φ is a three-variable function. Thus, it is more complicated than the μ^* correction given in [10] (where Φ is a two-variable function).

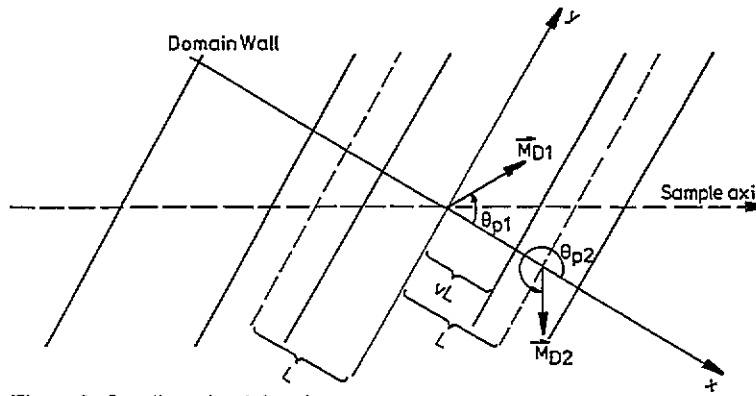

Figure 2. One-dimensional domain pattern.

2.4. Energy resulting from the magnetic poles on the walls

During the magnetization, the rotation of the domain magnetizations M_{D1} and M_{D2} from the domains joining the wall (figure 2) occurs, as well as the displacement of this wall. Let θ_{p1} and θ_{p2} be the angles between the normal n to the wall, and M_{D1} and M_{D2}, respectively. If the component of M_D normal to the wall is not continuous, charges appear on the wall surface, resulting in an increase in the magnetostatic energy. In order to evaluate this energy we shall use the general relation for the magnetostatic energy associated with the volume charges [11]. Choosing a coordinate system xOy so that $Ox \| n$ and Oy is parallel to the wall (figure 2), then

$$E_{mw} = \frac{\mu_0}{2} \sum_{n \neq 0} |M_n^x|^2 \left\{ 1 - \frac{1}{n\pi d/L} \left[1 - \exp\left(-n\pi \frac{d}{L} \right) \right] \right\}. \tag{8}$$

M_n^x is the x component of the Fourier coefficient M_n, and $2L$ is the spatial period of the one-dimensional domain structure. The x component of the magnetization is

$$M_x(x, y) = \begin{cases} M_D \cos\theta_{p1} & x \in (-vL,\ vL) \\ M_D \cos\theta_{p2} & x \in (-L,\ -vL) \cup (vL,\ L). \end{cases} \tag{9}$$

$M_x(x, y)$ can also be written as

$$M_x(x, y) = M_D(v\cos\theta_{p1}+(1-v)\cos\theta_{p2})+\sum_{n\neq 0} M_D(\cos\theta_{p1}-\cos\theta_{p2})\frac{\sin(\pi nv)}{\pi n}\exp\left(i\frac{n\pi x}{L}\right). \tag{10}$$

From equation (10) it follows that

$$M_n^x = M_D(\cos\theta_{p1} - \cos\theta_{p2})\frac{\sin(\pi nv)}{\pi n} \qquad \text{for } n \neq 0. \tag{11}$$

Taking into account equations (8) and (11), one obtains

$$E_{mw} = \frac{\mu_0}{2}M_D^2(\cos\theta_{p1} - \cos\theta_{p2})^2\sum_{n\neq 0}\frac{\sin^2(\pi nv)}{\pi^2 n^2}\left\{1 - \frac{1}{\pi nd/L}\left[1 - \exp\left(-\pi n\frac{d}{L}\right)\right]\right\}. \tag{12}$$

In the case of amorphous ribbons that have been field annealed, the domain width is $2L \simeq 200 \times 10^{-6}$ m. For $d/L \simeq 0.1$ and $v - \frac{1}{2} \ll 1$, one obtains

$$E_{mw} = c_1\frac{\mu_0}{2}M_D^2(\cos\theta_{p1} - \cos\theta_{p2})^2[1 - c_2(v - \tfrac{1}{2})^2] \tag{13}$$

where $c_1 = 0.05$, $c_2 = 1.4$. Thus

$$E_{mw} = \alpha_w(\cos\theta_{p1} - \cos\theta_{p2})^2[1 - c_2(v - \tfrac{1}{2})^2]. \tag{14}$$

The material parameter

$$\alpha_w = \frac{\mu_0}{2}c_1 M_D^2 \simeq 10^4 \text{J/m}^{-3} \tag{15}$$

is large compared with the value of the anisotropy constant. As the result of this interaction the magnetization process will occur so that the component of M_D normal to the wall is continuous.

2.5. The free-energy density; equilibrium conditions

The free-energy density F is

$$F = E_K + E_Z + E_V + E_V + E_S + E_{mw} + E_w \tag{16}$$

where E_K and E_Z are the densities of the anisotropy energy (equation (4)) and Zeeman energy, respectively [3]:

$$E_K = K[v\sin^2(\theta_1 - \epsilon) + (1 - v)\sin^2(\theta_2 - \epsilon)] \tag{17}$$

$$E_Z = -\mu_0 M_D H[v\cos\theta_1 + (1 - v)\cos\theta_2]. \tag{18}$$

E_V and E_S are given by equations (1) and (6). In order to express E_{mw} in terms of θ_1 and θ_2 and the wall direction γ (figure 1), we shall use the relations

$$\begin{aligned}\theta_{p1} &= \theta_1 - (\gamma - \pi/2)\\ \theta_{p2} &= \theta_2 - (\gamma - \pi/2).\end{aligned} \tag{19}$$

From (14) and (19) it follows that

$$E_{mw} = \alpha_w[\sin(\theta_1 - \gamma) - \sin(\theta_2 - \gamma)]^2[1 - c_2(v - \tfrac{1}{2})^2]. \tag{20}$$

E_w is the energy increase of the pinned wall during its bending:

$$E_w = 4\beta\sqrt{K}(v - \tfrac{1}{2})^2 \tag{21}$$

β being a material parameter; $\beta = (3L/d^2)\sqrt{A}$ [12], where A is the exchange constant.

To calculate the interesting parameters, it is necessary to expand the solutions to order H^2. We shall analyse two cases.

(a) Pinned wall ($\beta \neq 0$ and $\gamma = \epsilon$). In this case, the wall will not rotate and the balance equations are

$$\frac{\partial F}{\partial \theta_1} = \frac{\partial F}{\partial \theta_2} = \frac{\partial F}{\partial v} = 0. \tag{22}$$

The solutions will have the form

$$\begin{aligned} \theta_1 &= \epsilon + a_1 H + b_1 H^2 \\ \theta_2 &= \pi + \epsilon + a_2 H + b_2 H^2 \\ v &= \tfrac{1}{2} + a_3 H + b_3 H^2. \end{aligned} \tag{23}$$

The coefficients of the expansion (23) are

$$\begin{aligned} a_1 &= -a_2 \\ a_2 &= \frac{\mu_0 M_D(\alpha + \alpha_t + \beta\sqrt{K})\sin\epsilon}{2[(K+\alpha)(\alpha+\beta\sqrt{K}) + \alpha(K\sin^2\epsilon + \alpha + \beta\sqrt{K}\cos^2\epsilon)]} \\ a_3 &= \frac{\mu_0 M_D(\alpha + \alpha_t + K)\cos\epsilon}{2[(K+\alpha)(\alpha+\beta\sqrt{K}) + \alpha_t(K\sin^2\epsilon + \alpha + \beta\sqrt{K}\cos^2\epsilon)]} \end{aligned} \tag{24}$$

and

$$\begin{aligned} b_1 &= b_2 \\ b_2 &= \frac{\mu_0^2 M_D^2 \sin\epsilon\cos\epsilon}{2} \frac{1}{2(K+4\alpha_w)} \\ &\quad \times \frac{\beta\sqrt{K}(K+\alpha+\alpha_t)(\beta\sqrt{K}+\alpha+\alpha_t)}{[(K+\alpha)(\alpha+\beta\sqrt{K}) + \alpha_t(K\sin^2\epsilon + \alpha + \beta\sqrt{K}\cos^2\epsilon)]} \\ b_3 &= 0. \end{aligned} \tag{25}$$

Considering the conditions α_t and $\alpha_w \gg K_0$, it is found that

$$\begin{aligned} a_1 &= a_2 \\ a_2 &= \frac{\mu_0 M_D \sin\epsilon}{2(K\sin^2\epsilon + \beta\sqrt{K}\cos^2\epsilon + \alpha)} \\ a_3 &= a_2 \frac{\cos\epsilon}{\sin\epsilon} \end{aligned} \tag{26}$$

and

$$b_1 = b_2 = b_3 = 0. \tag{27}$$

In this case, the vectors M_{D1} and M_{D2} will rotate so that the bisectrix of the angle between the two vectors is normal to the pinned wall.

(b) Unpinned wall ($\beta = 0$ and $\gamma \neq \epsilon$). In this case, the wall may rotate and the balance equations are

$$\frac{\partial F}{\partial \theta_1} = \frac{\partial F}{\partial \theta_2} = \frac{\partial F}{\partial v} = \frac{\partial F}{\partial \gamma} = 0. \tag{28}$$

The solutions have the form

$$\begin{aligned}\theta_1 &= \epsilon + a_1' H + b_1' H^2 \\ \theta_1 &= \pi + \epsilon + a_2' H + b_2' H^2 \\ v &= \tfrac{1}{2} + a_3' H + b_3' H^2 \\ \gamma &= \epsilon + a_4' H + b_4' H^2.\end{aligned} \tag{29}$$

The coefficients $a_i' = a_i$ $(i = 1, 2, 3)$, $a_4' = 0$ and $b_i' = 0$ $(i = 1, 2, 3, 4)$. Therefore, for the two cases the coefficients of H are given by equation (26), the coefficients of H^2 are zero and $\gamma = \epsilon$ (the wall does not rotate). This is a consequence of both the magnetic domain coupling interaction and the shape effect. If $\alpha = \alpha_t = 0$ and $\alpha_w \gg K_0$, the vectors M_{D1} and M_{D2} will rotate so that $a_1 + a_2 \neq 0$ and $b_1 + b_2 \neq 0$. Thus, $\gamma = \epsilon + (\theta_1 + \theta_2 - \pi)/2 \neq \epsilon$.

2.6. The initial susceptibility

The initial susceptibility can be calculated starting from the expression for m_1 (equation (2)):

$$\chi = a_2 \sin\epsilon + 2a_3 \cos\epsilon. \tag{30}$$

Taking into account the relations (26), one gets

$$\chi(K_\sigma, \epsilon_0) = \frac{\mu_0 M_D^2}{2(K \sin^2\epsilon + \alpha + \beta\sqrt{K}\cos^2\epsilon)} \tag{31}$$

where K and ϵ depend on K_σ and ϵ_0 (see equation (5)). In figure 3 the dependence of the susceptibility on the magnetoelastic energy for various anneal angles ϵ_0 is presented. For the special cases $\epsilon_0 = 0$ and $\epsilon_0 = \pi/2$, a sharp peak appears. This happens for $K \simeq 0$ when, under the influence of the applied stress, a rotation of the easy axis of magnetization takes place. The susceptibility still has a finite value owing to the magnetostatic interactions.

Equation (31) describes both correlations of the type $\chi \propto K_\sigma^{-1}$ for high negative values of K_σ and of the type $\chi \propto K_\sigma^{-1/2}$ for high positive values of K_σ (pinned wall). This behaviour agrees with the experimental data reported in [13, 14].

For unpinned wall and transverse initial anisotropy the inverse susceptibility versus longitudinal stress (from equation (5) and (31)) is

$$\frac{1}{\chi(K_\sigma, \pi/2)} = \frac{2}{\mu_0 M_D^2}(|K_0 - K_\sigma| + \alpha) \qquad \text{for } K_\sigma < K_0 \tag{32}$$

and

$$\frac{1}{\chi(K_\sigma, \pi/2)} = \frac{2\alpha}{\mu_0 M_D^2} \qquad \text{for } K_\sigma > K_0 \tag{33}$$

which shows a plateau for $K_\sigma > K_0$. This behaviour was observed in Metglas 2605SC [2, 7].

In the case of the unstressed sample, the dependence of the normalized susceptibility on the field-annealing angle ϵ_0 is

$$\frac{\chi(0, \epsilon_0)}{\chi(0, 0)} = \frac{1}{1 + (c - 1)\sin^2\epsilon_0} \tag{34}$$

where

$$c = \frac{\chi(0, 0)}{\chi(0, \pi/2)} = \frac{K + \alpha}{\alpha}. \tag{35}$$

Equation (34) is different from the dependence given in [3] but agrees with the experimental data presented in [5] for VAC0040 (figure 4). The dependence given by equation (34) reflects the sample shape effect ($\alpha_t \gg K_0$).

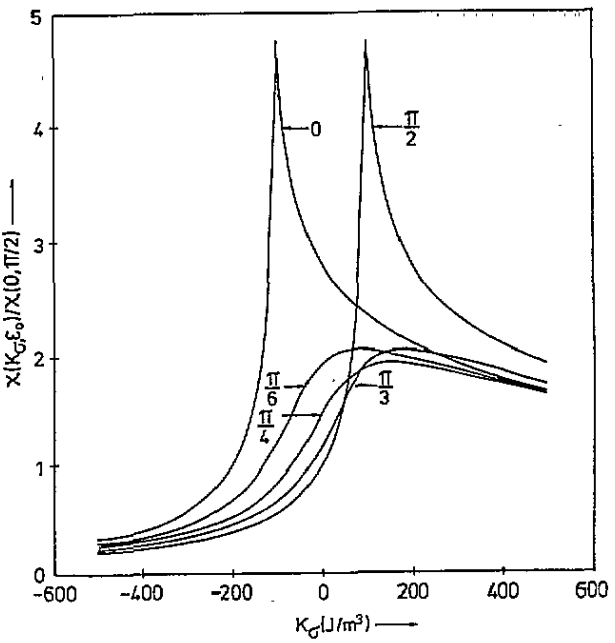

Figure 3. Normalized susceptibility at low fields against magnetoelastic anisotropy for various anneal angles. The values of the material parameters are $K_0 = 100$ J m^{-3}, $\alpha = 25$ J m^{-3} and $\beta = 2N^{1/2}$ m^{-1}.

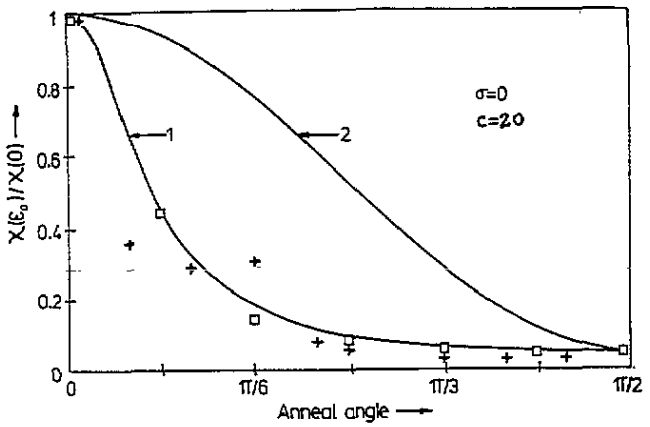

Figure 4. Normalized susceptibility at low fields against anneal: ——, curve 1, proposed model (equation (34)); ——, curve 2, Squire's [3] model; □, experimental data [5] for VAC0040; +, experimental data [5] for Metglas 2605S2.

2.7. Quadratic coefficients of engineering magnetostriction

The engineering magnetostriction λ_e is defined as the average axial strain of the sample [3]:

$$\lambda_e = \tfrac{3}{2}\lambda_s[v\cos^2\theta_1 + (1-v)\cos^2\theta_2 - \cos^2\epsilon].$$

For low fields (taking into account equation (23)) one obtains

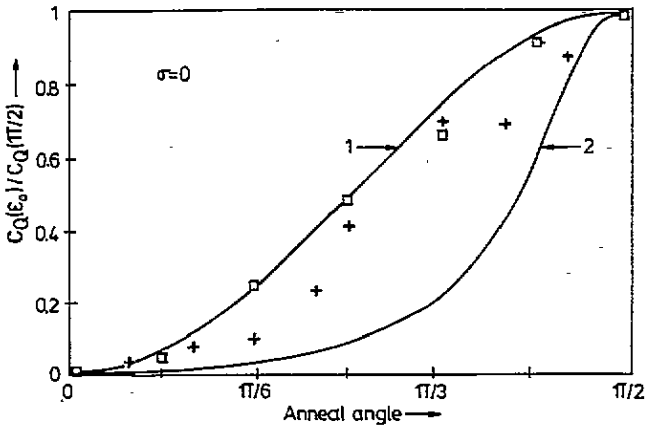

Figure 5. Normalized intrinsic quadratic coefficient against anneal angle: ——, curve 1, proposed model (equation (38)); ——, curve 2, Squire's [3] model; □, experimental data [5] for VAC0040; +, experimental data [5] for Metglas 2605S2.

$$\lambda_e = \tfrac{3}{2}\lambda_s \left[-a_2^2 \cos(2\epsilon) + \left(2a_2 a_3 - \frac{b_1 + b_2}{2} \right) \sin(2\epsilon) \right] H^2. \tag{36}$$

Thus, at low applied fields H, or low levels of technical magnetization M, the magnetostrictive strain λ_e is given by

$$\lambda_e \propto H^2 \propto M^2.$$

The response can be parametrized by the quadratic coefficients c_q and C_Q

$$\lambda_e = c_q H^2$$

$$\lambda_e = C_Q M^2.$$

The constants c_q and C_Q of proportionality in the above expression are called the *quadratic coefficient of magnetostriction* (or *quadratic coefficient*) and *intrinsic quadratic coefficient*, respectively [3]. Taking into account equations (26), (27) and (36), one obtains

$$c_q(K_\sigma, \epsilon_0) = \frac{3}{8}\lambda_s \frac{\mu_0^2 M_D^2}{(K+\alpha)^2} \left(\frac{c \sin\epsilon}{1 + (c-1)\sin^2\epsilon} \right)^2 \tag{37}$$

$$C_Q(K_\sigma, \epsilon_0) = \frac{3}{2}\frac{\lambda_s}{M_D^2} \sin^2\epsilon. \tag{38}$$

The dependences $\epsilon(K_\sigma, \epsilon_0)$ and $K(K_\sigma, \epsilon_0)$ are given by equation (2). Figure 5 presents the dependence of the normalized intrinsic quadratic coefficient on the easy axis direction given by equation (38), the dependence given by Squire's [3] model and the experimental data presented in [5]. The proposed model agrees with the experimental data for VAC0040. The dependence $C_Q(0, \epsilon_0)$ reflects the shape effect and the magnetostatic interaction due to the magnetically charged wall for a pinned wall ($\alpha_w \gg K_0$). The magnetoelastic anisotropy dependence of the intrinsic quadratic coefficient $C_Q(K_\sigma)$, for various anneal angles, is present in figure 6 (equation (38)). The maximum values are obtained for resulting transverse anisotropy ($\epsilon = \pi/2$). The discontinuities for $\epsilon_0 = 0$ and $\epsilon_0 = \pi/2$ are consequences of the sudden changes in the easy axis direction for $K_\sigma = -K_0$ and $K_\sigma = K_0$, respectively.

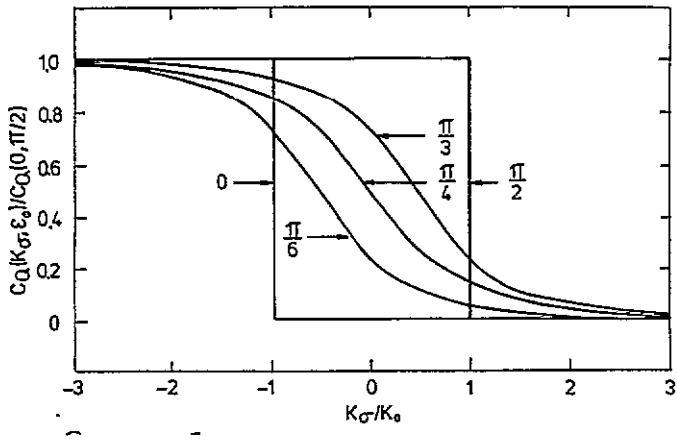

Figure 6. The magnetoelastic anisotropy dependence of the normalized intrinsic quadratic coefficient for various anneal angles (equation (38)).

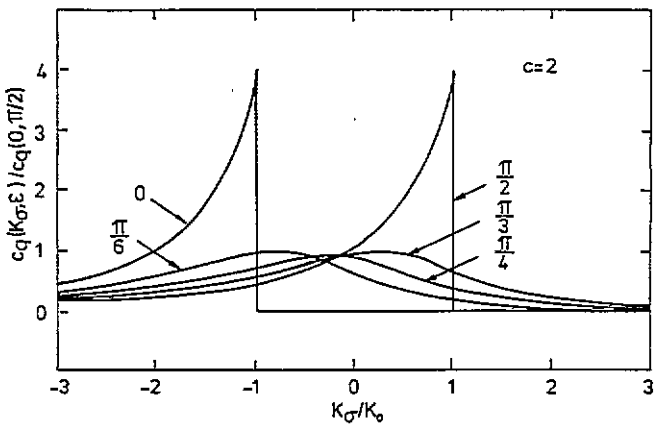

Figure 7. The magnetoelastic anisotropy dependence of the normalized quadratic coefficient for various anneal angles (equation (37)).

Figure 7 presents the dependences of the quadratic coefficient $c_q(K_\sigma)$ on the magnetoelastic anisotropy for various anneal angles (equation (37)). In the case $\epsilon_0 = \pi/2$, the maximum value of c_q was observed experimentally for $K_\sigma = K_0$ [15]. The proposed model gives a finite value in this case too.

The dependence of the intrinsic quadratic coefficient on the field-annealing angle reflects the shape effect and the influence of the magnetostatic interaction due to the magnetically charged wall for a pinned wall.

3. Conclusions

An important part in the magnetic and magnetoelastic behaviour of the amorphous ribbons in weak magnetic field is played by the shape effect (the transverse demagnetizing field requires alignment of the technical magnetization along the sample) and the effect produced

by the magnetic charges on the wall surface. This interaction will result in the coupling between the wall direction and the magnetization directions within the joining domains, M_{D1} and M_{D2}. The reorientation of M_{D1} and M_{D2} will occur so as to maintain the component normal to the wall. The energies due to the shape effect and poles on the walls are much greater than the intrinsic anisotropy energy.

The ribbon shape effect is reflected in the dependence of the initial susceptibility on the direction of the easy axis.

The dependences of the quadratic coefficients of engineering magnetostriction on the field-annealing angle reflect the shape effect and the influence of the magnetostatic interaction due to the magnetically charged wall for pinned wall.

When the resulting anisotropy vanishes, the magnetic domain coupling interaction opposes the tendency of the adjacent domain magnetizations to align parallel to the applied field, which results in finite values of the susceptibility and quadratic coefficient in these cases too.

References

[1] Livingstone J D 1982 *Phys. Status Solidi* a **70** 591
[2] Savage H T and Spano M L 1982 *J. Appl. Phys.* **53** 8092
[3] Squire P T 1990 *J. Magn. Magn. Mater.* **87** 299
[4] Sablik M J and Jiles D C 1993 *IEEE Trans. Magn.* **MAG-29** 2113
[5] Thomas A T and Gibbs M R J 1992 *J. Magn. Magn. Mater.* **103** 97
[6] Ciobotaru I 1995 *J. Magn. Magn. Mater.* in press
[7] Chiriac H and Ciobotaru I 1993 *J. Magn. Magn. Mater.* **124** 277
[8] Chiriac H, Ciobotaru I and Mohorianu S 1994 *IEEE Trans. Magn.* **MAG-30** 518
[9] Joseph R J and Schlomann E 1965 *J. Appl. Phys.* **36** 1579
[10] Chikazumi S 1964 *Physics of Magnetism* (New York: Wiley)
[11] Corciovei A and Adam Gh 1971 *J. Physique Coll.* **32** C1 408
[12] Luborsky F E 1983 *Amorphous Metallic Alloys* ed F E Luborsky (London: Butterworth) p 372
[13] Aroca C, Sanchez P S and Lopez E 1981 *IEEE Trans. Magn.* **MAG-17** 1462
[14] Hayashi K, Hayakawa M, Ochiai Y, Matsuda H, Ishikawa W and Aso K 1984 *J. Appl. Phys.* **55** 3028
[15] Bucholtz F, Koo K P, Yurek A M, McVicker J A and Dandridge A 1987 *J. Appl. Phys.* **61** 3790